Functional Characterization of Pediocin PA-1 Binding to Liposomes in the Absence of a Protein Receptor and Its Relationship to a Predicted Tertiary Structure†

YUHUAN CHEN,[1] RONI SHAPIRA,[2] MIRIAM EISENSTEIN,[3] AND THOMAS J. MONTVILLE[1]*

Department of Food Science, New Jersey Agricultural Experiment Station, Cook College, Rutgers, The State University of New Jersey, New Brunswick, New Jersey 08903-0231,[1] and Institute of Biochemistry, Food Science and Nutrition, Faculty of Agriculture, The Hebrew University of Jerusalem,[2] and Department of Structural Biology, Weizmann Institute of Science,[3] Rehovot 76100, Israel

The physicochemical interaction of pediocin PA-1 with target membranes was characterized using lipid vesicles made from the total lipids extracted from *Listeria monocytogenes*. Pediocin PA-1 caused the time- and concentration-dependent release of entrapped carboxyfluorescein (CF) from the vesicles. The pediocin-induced CF efflux rates were higher under acidic conditions than under neutral and alkaline conditions and were dependent on both pediocin and lipid concentrations. A binding isotherm constructed on the basis of the Langmuir isotherm gave an apparent binding constant of 1.4×10^7 M^{-1} at pH 6.0. The imposition of a transmembrane potential (inside negative) increased the CF efflux rate by 88%. Pediocin PA-1 also permeablized synthetic vesicles composed only of phosphatidylcholine. Sequence alignments and secondary-structure predictions for the N terminus of pediocin PA-1 and other class IIa bacteriocins predicted that pediocin PA-1 contained two β-sheets maintained in a hairpin conformation stabilized by a disulfide bridge. The structural model also revealed patches of positively charged residues, consistent with the argument that electrostatic interactions play an important role in the binding of pediocin PA-1 to the lipid vesicles. This study demonstrates that pediocin PA-1 can function in the absence of a protein receptor and provides a structural model consistent with these results.

Four classes of antimicrobial peptides or proteins, termed bacteriocins, can be ribosomally synthesized by various lactic acid bacteria (LAB) (28). Pediocin PA-1 is representative of the rapidly expanding family of class IIa, or pediocin-like, bacteriocins, which contain a YGNGV consensus motif near the N terminus of the cationic peptide and conventional disulfide bonds rather than lanthionine rings (25). Class IIa bacteriocins constitute the majority of LAB bacteriocins (24) and are produced by a number of LAB genera usually associated with meats. In addition to pediocin PA-1 (23), which has total sequence identity with pediocin AcH (40), examples of class IIa bacteriocins which have been extensively characterized are leucocin A (22), bavaricin MN (27), carnobacteriocin BM1 (46), and enterocin A (4).

The use of bacteriocins as a part of a multiple-component preservation system against food-borne pathogenic and spoilage microorganisms is attractive to the food industry (30). The pediocin-like bacteriocins and their producing strains kill the psychrotrophic pathogen *Listeria monocytogenes* not only in laboratory broth cultures but also in model food systems, especially meat products where nisin fails to work (39, 45). The use of pediocin PA-1 in the preservation of various foods such as cheeses, meats, and salads is covered by European patents (20, 53).

The primary structure of pediocin PA-1 has been determined by Edman degradation of the purified peptide (23) and by sequence analysis of the structural gene (35, 40). It consists of 44 amino acids with a molecular weight (MW) of 4,629. The

disulfide bonds, in particular the bond between residues 24 and 44, are essential for pediocin PA-1's action against sensitive *Pediococcus* cells and membrane vesicles (10) and *Listeria* cells (9). The action involves the formation of a poration complex in the target membrane, which results in efflux of small intracellular substances, depletion of cytoplasmic ATP, dissipation of proton motive force, and ultimately cell death (8, 25). Although only limited studies have been conducted on the detailed mechanism of action of class IIa bacteriocins, several investigators have suggested that membrane-associated receptor proteins are required for the function of pediocin PA-1, lactococcin A, and other class IIa bacteriocins (1, 10, 55). While nuclear magnetic resonance (NMR) data and computer simulation studies demonstrate that nisin has a flexible structure in aqueous solution and several constrained regions in membrane-mimicking environments (33, 43, 54), little is known about the secondary and tertiary structures of class IIa bacteriocins (25), except for leucocin A. Data from NMR studies indicate that leucocin A exists as a random coil in water, while in membrane-mimicking solvents an amphiphilic helical region is present in the C-terminal section after the loop maintained by a disulfide bond (49). As with other class IIa bacteriocins, the three-dimensional structure of pediocin PA-1 and its relationship to pediocin action are unknown.

This paper reports the physicochemical interaction of pediocin PA-1 with vesicles made from lipids extracted from *L. monocytogenes* cell membranes and presents a structural model consistent with binding in the absence of a protein receptor. Pediocin PA-1 also permeablized vesicles composed only of synthetic phospholipids, further proving that pediocin PA-1 has no absolute requirement for a protein receptor. Pediocin PA-1's predicted tertiary structure contains patches of positive charge which could allow it to interact directly with phospho-

* Corresponding author. Phone: (908) 932-9611, ext. 218. Fax: (908) 932-6776. E-mail: montville@aesop.rutgers.edu.

lipid head groups which might serve as functional bacteriocin binding sites in the absence of protein receptors.

MATERIALS AND METHODS

Purification of pediocin PA-1. The pediocin PA-1-producing strain *Pediococcus acidilactici* PAC 1.0 was grown in Lactobacilli MRS (Difco) broth with 0.6% yeast extract at 30°C for 20 to 22 h. Culture supernatant was obtained by centrifugation, followed by filtration using a 0.45-μm-pore-size membrane filter (Gelman Sciences, Ann Arbor, Mich.) to remove cells. Pediocin activity was measured in arbitrary units (AU) as previously described (45).

Pediocin PA-1 was purified by the method of Chikindas et al. (10). Briefly, the cell-free supernatant was precipitated by 50% (vol/vol) ethanol, resuspended in 50 mM 2-(*N*-morpholino)-ethanesulfonate (MES) buffer (pH 6.0), and dialyzed against distilled water in dialysis tubing (Spectrum, Houston, Tex; MW cutoff, 1,000) to obtain a low-ionic-strength protein preparation. The preparation was purified by preparative isoelectric focusing using a Rotofor cell (Bio-Rad Laboratories, Melville, N.Y.). To minimize protein precipitation, 5.0 M urea (enzyme grade) and 10% glycerol were included in the running buffer containing 1% ampholytes (Bio-Lyte 3/10). Active fractions with pI > 9.5 were pooled, mixed with NaCl (1.0 M, final concentration), and dialyzed against MES buffer. During dialysis, the pediocin preparation was concentrated up to twofold by coating the dialysis tubing with polyethylene glycol (average MW, 10,000). Protein concentration was determined with a modified Bradford method (Coomassie Plus assay; Pierce, Rockford, Ill.), using bovine serum albumin as the standard. The purity of the sample was determined by sodium dodecyl sulfate-polyacrylamide gel electrophoresis. This purification scheme resulted in a single silver-stained band.

Growth of *L. monocytogenes* and isolation of lipids. *L. monocytogenes* Scott A cells were grown at 30°C to mid-exponential phase (A_{660} = 0.6 to 0.8) in Trypticase soy broth containing 0.5% dextrose and 0.6% yeast extract. After washing once with 0.1% peptone, lipids were extracted by the procedure of Bligh and Dyer (41) with some modifications (56).

Preparation of lipid vesicles. Large unilamellar vesicles composed of lipids from *L. monocytogenes* were prepared as described by Winkowski et al. (56). The lipids dissolved in chloroform-methanol were dried under a stream of N_2 gas in a siliconized microcentrifuge tube. Residual solvent was removed by centrifugation under vacuum for 2 h. The dried lipids were resuspended in MES buffer containing *n*-octyl-β-D-glucopyranoside and 50 mM 5(6)-carboxyfluorescein (CF) to a final lipid concentration of 6 to 10 mg/ml. The molar ratio of *n*-octyl-β-D-glucopyranoside to lipids was approximately 14:1. After repeated vortexing for 1 h, the lipid-CF-detergent mixture was passed through a Sephadex G-50 superfine column (0.7 by 10 cm) which had previously been equilibrated with MES buffer and 0.4 ml of 50 mM CF to enhance dye entrapment. CF-loaded lipid vesicles eluted in the void volume, while the octylglucoside and untrapped CF were retained in the column. The vesicles were stored on ice for up to 3 h until use. CF-loaded vesicles were also made with 50 mM MES buffer at pH 5.5, 6.5, 7.0, or 7.5 under otherwise identical conditions described above. Plain lipid vesicles were made in the absence of CF under otherwise identical conditions as for the preparation of CF-loaded vesicles.

Phospholipid vesicles composed of 1-palmitoyl-2-oleoyl-*sn*-glycero-3-phosphocholine (POPC; Avanti, Alabaster, Ala.) were prepared as follows: 6 mg of POPC in chloroform was dried, resuspended in 1 ml of MES buffer containing 40 mM CF, pipette mixed, and freeze-thawed for five cycles in solid CO_2-ethanol. The mixture was then sonicated for 30 s at 30 W to obtain large unilamellar vesicles (15), using a sonifier from Branson (Plainview, N.Y.). Untrapped CF was removed by passing the mixture through a Sephadex G-50 superfine column (0.7 by 10 cm) equilibrated with MES buffer. The CF-loaded lipid vesicles again eluted in the void volume. The phospholipid concentration of vesicles was determined by the Bartlett assay as described by New (41).

CF leakage assay. The ability of pediocin PA-1 to cause CF release from lipid vesicles was determined by monitoring the increase in fluorescence of the vesicle solution upon additions of various concentrations of pediocin PA-1 as previously described (27, 56). Maximal CF leakage was determined by the addition of the detergent Triton X-100 (final concentration, 0.2%, vol/vol). Progress of the CF efflux was expressed as the percentage of CF release, calculated from the equation % efflux = $[(F_t - F_0)/(F_\infty - F_0)]100$, where F_t was the fluorescence at time t, F_0 was the control fluorescence at time t, and F_∞ was the fluorescence after Triton X-100 addition. The controls were done by adding, instead of pediocin PA-1, its diluent (the MES buffer used to prepare pediocin PA-1) or valinomycin and ethanol when appropriate. The control levels were subtracted from the fluorescence levels caused by pediocin PA-1. Rates of CF efflux (percent per minute) were calculated from the slope of a tangent to the efflux curve at 120 s after the addition of pediocin PA-1.

To determine whether pediocin PA-1 induced gross structural changes (such as fusion or aggregation) of the lipid vesicles, changes in 90°C light scattering of the vesicle solution were determined with a spectrofluorometer (model F1T11; Spex Industries, Metuchen, N.J.). A wavelength of 400 nm and band pass slit settings of 4 nm were used. The predicted magnitude of increase in light scattering without gross structural changes was calculated as described by Grant et al. (21).

Imposition of membrane potential. An artificial membrane potential was generated by a valinomycin-mediated outward potassium diffusion gradient (27, 52).
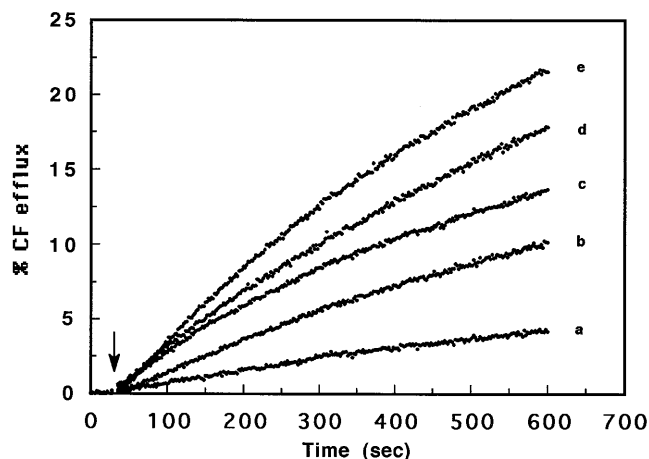

FIG. 1. Pediocin PA-1-induced CF efflux from lipid vesicles derived from *L. monocytogenes* Scott A at pH 6.0. The pediocin concentrations were 1.3 (a), 2.5 (b), 3.8 (c), 6.3 (d), and 12.5 (e) μg/ml. The lipid concentration was 8.3 μM. The arrow indicates the time of pediocin additions.

Briefly, *Listeria* lipid vesicles were prepared in Na-MES buffer (50 mM, pH 6.0) containing 5 mM KH_2PO_4. After eluting from the gel filtration column, the vesicles were centrifuged and washed once in either 5 or 0.05 mM KH_2PO_4 and resuspended in the buffer that they were washed in. This created a theoretical membrane potential (Δψ), after the addition of valinomycin to generate the gradient, across the vesicle membrane of either 0 or 120 mV (inside negative). The vesicles were stored on ice until use for up to 1.5 h. The CF efflux assay was performed as described above except that 2.5 μM valinomycin (in 95% ethanol, final concentration) was added to the vesicle solution (2 ml of Na-MES buffer containing 5 or 0.05 mM KH_2PO_4) 10 to 15 s prior to the addition of the control, Triton X-100, or pediocin PA-1.

Structural modeling. To identify proteins with sequences similar to that of pediocin PA-1, the SwissProt database was subjected to a FastaA search with the Smith-Waterman algorithm (51). The Smith-Waterman algorithm was then used to align the sequences. The methods referenced in Table 3 were used to predict secondary structure based on single and multiple sequence alignments. Threading programs (7, 26, 50) were applied to the pediocin PA-1 sequence to identify a known structure in the Protein Data Bank (7) that could be used as a template for tertiary-structure model building.

Culture media and reagents. Trypticase soy broth was from BBL Microbiology Systems (Cockeysville, Md.). All other media were purchased from Difco Laboratories (Detroit, Mich.). MES buffer was from Research Organics Inc. (Cleveland, Ohio). Polyethylene glycol, CF, octylglucoside, valinomycin, and the Sephadex G-50 superfine resin were from Sigma Chemical Co. (St. Louis, Mo.). All other reagents, except otherwise specified, were purchased from Fisher Scientific Co. (Pittsburgh, Pa.).

RESULTS AND DISCUSSION

Physicochemical characterization of pediocin PA-1-induced CF efflux from lipid vesicles. Exposure to pediocin PA-1 caused the gradual release of CF from *Listeria* lipid vesicles at pH 6.0. The CF efflux was both time dependent and pediocin concentration dependent (Fig. 1). At a low pediocin concentration of 1.3 μg/ml, CF efflux tended to plateau at 600 s, while at 6.3 μg/ml, the efflux continued to increase at 900 s, although at a decreasing rate (data not shown). Once the vesicles had been treated with pediocin PA-1, successive addition of the bacteriocin caused additional CF leakage only when the initial pediocin concentration was less than 2.5 μg/ml. Both the efflux rate and the overall percentage of efflux at 600 s increased with increasing pediocin concentrations.

Light scattering results suggested that under the conditions used in this study, binding of the pediocin molecules did not cause gross structural changes of the vesicles. The observed light scattering values upon pediocin-vesicle interaction were substantially smaller than the ones predicted for fusion or aggregation (Table 1). Therefore, the CF efflux resulted from

TABLE 1. Light scattering of lipid vesicles[a] exposed to pediocin PA-1

[Pediocin][b] (μM)	Change in ic/iv		
	Predicted		Observed
	Without fusion or aggregation	With fusion or aggregation[c]	
5.0 μM Lipids			
0.26	1.56–1.77	>3.12	1.30
0.52	2.27–2.75	>4.54	1.58
25.0 μM Lipids			
0.26	1.10–1.14	>2.20	1.09
0.52	1.21–1.28	>2.42	1.19
1.05	1.43–1.59	>2.87	2.62
2.10	1.94–2.33	>3.70	2.97

[a] The relative increase in 90° light scattering (ic/iv) was determined at pH 6.0; ic and iv stand for light intensity of pediocin-vesicle complexes and vesicle control, respectively.

[b] Pediocin (0.26 to 2.1 μM) was added to vesicle solutions containing either 5.0 or 25.0 μM *Listeria* lipids.

[c] Lower limit estimated, assuming all peptide-vesicle complexes double in mass. The values were obtained by multiplying the smaller number in the previous column by 2.

the interaction of pediocin PA-1 molecules with individual lipid vesicles.

Pediocin PA-1 caused CF leakage from lipid vesicles composed of total lipids extracted from *L. monocytogenes* Scott A, in agreement with its action in vivo, where pediocin PA-1 permeablizes the cellular cytoplasmic membrane and causes the release of intracellular potassium and inorganic phosphate (9). Pediocin PA-1 action is consistent with pore formation, which is generally accepted as the mechanism by which bacteriocins from LAB function in target membranes (1, 10, 17, 25, 28, 34, 42, 52) rather than a nonspecific detergent-like action. Pediocin PA-1-induced CF efflux was gradual and followed saturation kinetics. This is inconsistent with the rapid all-or-none action of detergents. The *Listeria* lipid vesicles were treated with a detergent (Triton X-100) at the end of each assay to obtain a 100% efflux value which was used to normalize the data. The addition of Triton X-100 rapidly disrupted the lipid vesicles within seconds. This would have not occurred in vesicles which had already been permeablized by a detergent. Moreover, pediocin PA-1 denatured by a reducing agent is inactive and does not deplete ATP or induce efflux of K^+ and P_i from *L. monocytogenes* cells (9). The concentrations of pediocin PA-1 used in this study were similar to those used in studies of bavaricin MN (27), nisin (17, 56), and magainin 2 (36, 38) where the antimicrobial peptides formed pores in the target membrane at 0.2 to 3.0 μM peptide concentrations.

Since the lipid vesicle system used in this study is devoid of membrane proteins (56), the results from this study strongly suggest that a protein receptor was not required for the recognition and binding of pediocin PA-1 to the *Listeria* membranes. Instead, the pediocin molecules may recognize particular membrane (phospho)lipids, as has been suggested for the mode of action of mesentaricin Y105, a pediocin-like bacteriocin (34). Alternatively, pediocin PA-1 might bind to the membrane surface because of electrostatic interaction between the positively charged pediocin molecule and the negatively charged phospholipid head groups.

To further exclude an absolute requirement for a membrane protein receptor, which could have been present as an undetectable contaminant in the *Listeria* lipid vesicles, we investigated the effect of pediocin PA-1 on lipid vesicles made from

a synthetic phospholipid. CF-loaded lipid vesicles were made by using POPC. The additions of pediocin PA-1 resulted in CF efflux from the POPC vesicles (Fig. 2). The efflux from POPC vesicles was even more rapid than from *Listeria* vesicles and tended to plateau sooner (at 200 s) after pediocin additions. The POPC vesicles were sensitive to nisin at a concentration much lower than the pediocin concentrations used. Previous studies on pediocin PA-1 and lactococcin A suggest that they require a protein receptor in the target membrane to function (10, 52, 55). In the same study, Chikindas et al. (10) found that pediocin PA-1 binds to and inserts (not deeply) in *Escherichia coli* lipid vesicles without a protein receptor. In this study, CF efflux was induced by pediocin PA-1 from complex *Listeria* lipid vesicles as well as from simple vesicles composed only of POPC. The fact that CF leakage from both types of vesicles was pediocin concentration dependent definitively established that pediocin PA-1 permeablized the lipid vesicles in the absence of protein receptors.

The degree of membrane permeabilization induced by pediocin PA-1 depended not only on pediocin concentration but also on lipid concentration (Fig. 3A). The pediocin dose-response curves for the efflux rate at different lipid concentrations were constructed to quantitatively evaluate the affinity of the peptide to the vesicles. The binding affinity constant was determined according to the procedures described for other membrane-active antimicrobial peptides (12, 21, 37, 56). The initial rate of CF efflux was a function of pediocin concentration at a given lipid concentration. This indicated that the [pediocin]/[lipid] ratio influenced CF efflux. As the concentration of lipid increased, for example, from 5.2 to 49.9 μM, a greater amount of pediocin PA-1 was needed to cause the same efflux rate. More precisely, the concentration of membrane-bound peptide was increased with increasing lipid concentration to yield a constant efflux rate, which was represented by a linear function (Fig. 3B). The *y* intercept (concentration of free pediocin, [P_f]) and the slope (ratio of membrane-bound pediocin per lipid, *r*) of each curve were used as a datum point to construct the binding isotherm (Fig. 3C). On the basis of geometry, 51% of the total lipids were in the outer leaflet of the vesicle bilayer and available for pediocin binding, since the mean diameter of the CF-loaded vesicles was 440 nm (56). Therefore, *r* = r/0.51 instead of *r* was used to construct the isotherm. Analysis of the isotherm according to the Langmuir
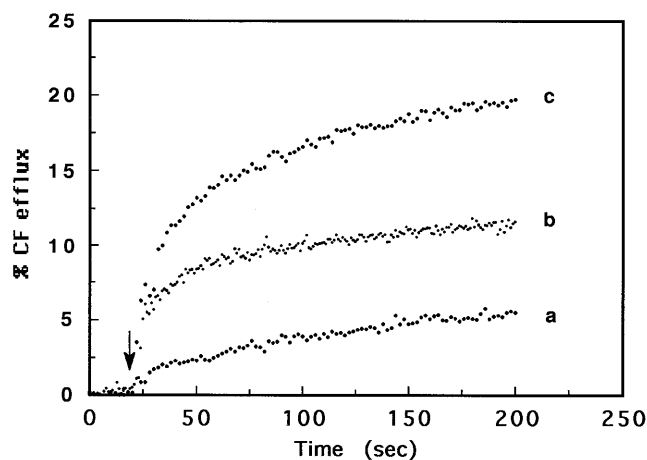

FIG. 2. CF efflux from lipid vesicles composed of POPC. (a) Pediocin PA-1 at 6.3 μg/ml; (b) pediocin PA-1 at 18.9 μg/ml; (c) nisin at 1.5 μg/ml. The lipid concentration was 25.3 μM. The arrow indicates the time of bacteriocin additions.

FIG. 4. Relationship between efflux rate and the molar ratio of bound pediocin and total lipid (r) at pH 6.0. The intercept at the x axis represents the critical number of pediocin PA-1 molecules per mole of *Listeria* lipid required to initiate CF efflux.
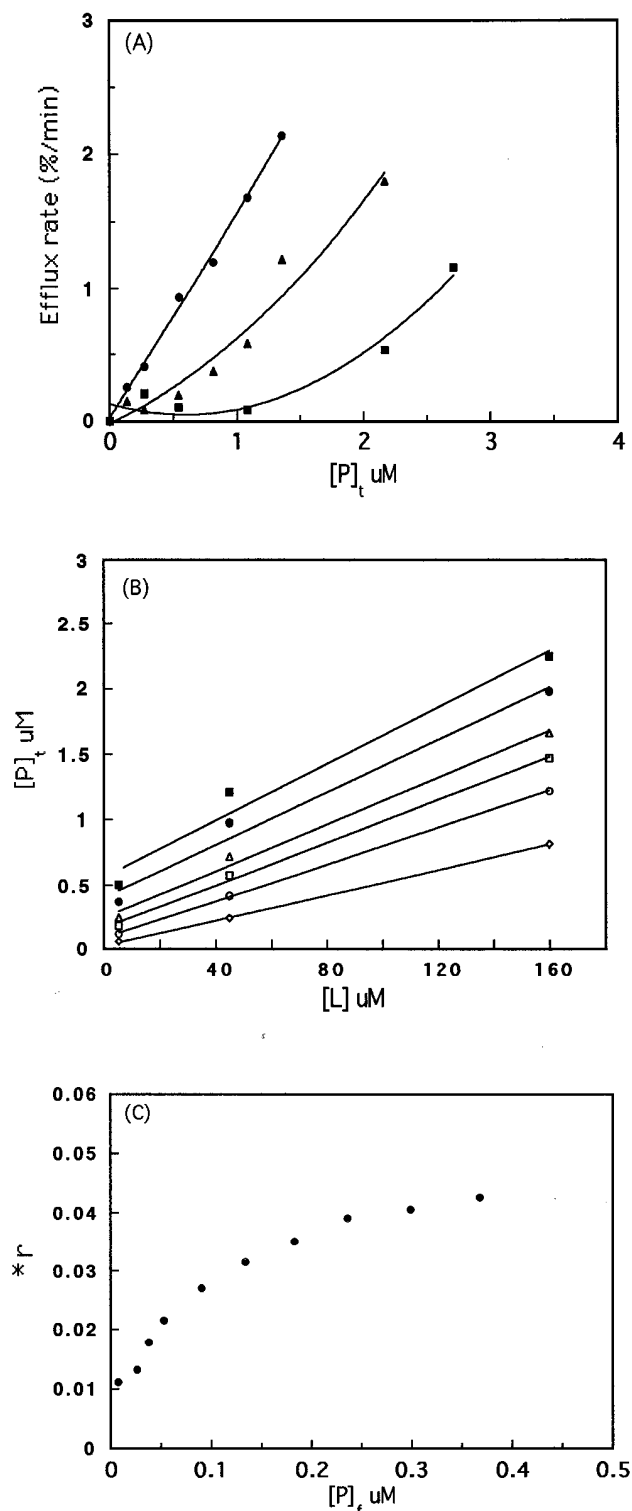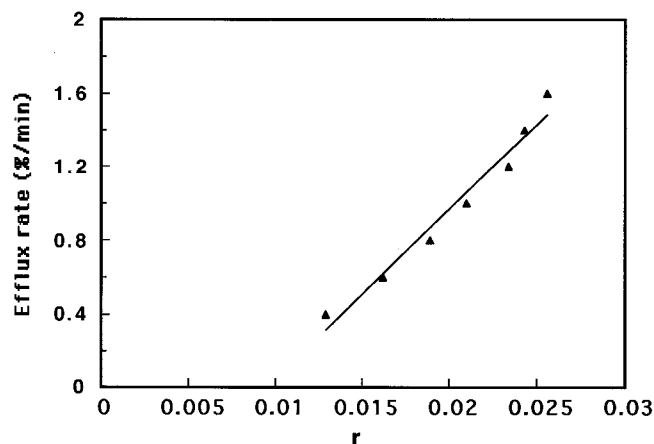

FIG. 3. Construction of a binding isotherm for the interaction of pediocin PA-1 with CF-loaded *Listeria* lipid vesicles at pH 6.0. (A) Initial efflux rate as a function of total pediocin PA-1 concentration ([P]$_t$) at three lipid concentrations: 5.2 μM (●), 49.9 μM (▲), and 159.9 μM (■). (B) Linear relationship between lipid concentration ([L]) and [P]$_t$ according to the defined equation $[P]_t = [P]_f + r[L]$, where [P]$_f$ and r represented the concentration of free pediocin and the slope of the curve, respectively. Curves from the bottom to the top represent efflux rates of 0.1, 0.2, 0.3, 0.4, 0.6, and 0.8%/min, respectively. (C) Binding isotherm. The binding affinity constant was obtained by fitting the datum points to the Langmuir equation $*r = (nk[P]_f)/(1 + k[P]_f)$. $*r$ equals $r/0.51$, based on a vesicle diameter of 440 nm, k is the apparent binding concentration, and n is the maximum number of lipid binding sites.

binding equation resulted in an apparent binding constant of $(1.4 \pm 0.3) \times 10^7$ M^{-1}. The number of binding sites per lipid molecule was estimated as 0.04 ± 0.01; thus, about 25 lipid head groups constituted a functional binding site for a pediocin PA-1 molecule.

The relationship between the CF efflux rate and the molar ratio of bound peptide per lipid (r) is shown in Fig. 4. A critical r value of around 0.01 was required to initiate efflux at pH 6.0. This value is in the same order of magnitude as the one estimated for nisin (56). On the other hand, the binding affinity of pediocin PA-1 was an order of magnitude higher than the value determined for nisin with the same *Listeria* lipid vesicle system. This suggests that pediocin PA-1 binds to the lipid vesicles more strongly than nisin does. The pediocin PA-1 molecule has a net charge of +7 at pH 6.0, while nisin's net charge is +5. Furthermore, the two disulfide bonds of pediocin PA-1 would bring the positively charged Lys and His residues closer together (see the three-dimensional structural model shown below) to form clusters of positively charged side chains which may anchor the pediocin molecule more tightly to the negatively charged lipid head groups on the surface of the vesicle bilayer and thus decrease the dissociation rate of bound pediocin. Other antimicrobial peptides such as magainin 1 and magainin 2 interact with acidic phospholipids through electrostatic interactions, followed by pore formation to induce leakage (36–38). A model study of nisin-membrane interactions which used lipid monolayers concluded that ionic interactions, especially of the positively charged residues of nisin's C terminus with negatively charged lipid head groups, play a major role in nisin Z binding (14). This is because nisin has strong affinity with anionic lipids but very weak affinity with zwitterionic or neutral lipids.

It is puzzling, however, that even though pediocin PA-1 had a higher affinity to the lipid vesicles than nisin at pH 6.0, it caused a lower CF efflux rate at a [peptide]/[lipid] ratio similar to that of nisin. This prompted us to investigate other factors that influence pediocin PA-1 insertion and pore formation, in light of the hypothesis that pediocin PA-1 increases the permeability of target membranes through a multistep process consisting of binding, insertion, and pore formation (42).

Influence of pH and membrane potential on pediocin PA-1. The rate of CF efflux induced by pediocin PA-1 was pH dependent (Fig. 5). The initial efflux rates were higher at acidic
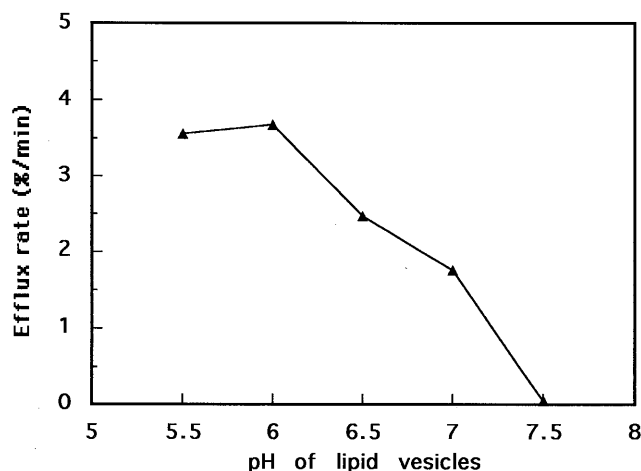
FIG. 5. Influence of pH on pediocin-induced CF efflux rate at a pediocin concentration of 6.3 µg/ml. CF-loaded vesicles at each pH were prepared with 3 mg of dried listeria lipids. The final lipid concentrations ranged from 4.7 to 8.3 µM. See Materials and Methods for details.

pH than at alkaline pH. There was little efflux at pH 7.5. As the pH decreased to neutral and acidic levels, the efflux rate increased and reached about 3.7%/min at pH 6.0. A similar level was observed for pH 5.5. Because of the poor solubility of CF below pH 5.5, efflux at pH <5.5 could not be determined.

Bacteriocins are positively charged under physiological conditions due to the presence of basic residues such as His and Lys. The buffer pH affects the ionization of the side chains and hence influences the interaction of the peptide with the membrane. Nisin induces an increase in CF efflux from *Listeria* lipid vesicles as the pH increases from pH 5.0 to 8.0 (56). This increase is attributed to the deprotonation of nisin's two His residues, which enhances nisin insertion into the membrane. It is interesting that alkaline pH was inhibitory to pediocin PA-1. This suggests that the deprotonation of pediocin's three His residues does not play as an important role in its insertion. In contrast, the protonation of the His residues might contribute significantly to the binding of pediocin to the membrane, since decreasing the pH from 7.5 to 5.5 caused a corresponding increase in the CF efflux rate. This interpretation is supported by the observation that for bavaricin MN, which like pediocin PA-1 contains four Lys residues but which lacks His, the optimal pH for efflux is 6.0. Bavaricin's CF efflux rate decreases as pH moves from the optimum (27).

The effect of a transmembrane potential ($\Delta\psi$) on pediocin-induced CF efflux was studied by preparing lipid vesicles with potassium MES buffer and diluting the potassium-loaded vesicles 100-fold in sodium MES buffer in the presence of valinomycin. The presence of a $\Delta\psi$ (inside negative) dramatically enhanced the action of pediocin PA-1 (Fig. 6). The initial CF efflux rate produced by pediocin in the presence of a membrane potential (-120 mV) was 10.5%/min, which was 88% higher than in its absence. The magnitude of the $\Delta\psi$-mediated increase in CF efflux is similar to that reported previously (27) for another pediocin-like bacteriocin, bavaricin MN (66% increase in the presence of -120-mV $\Delta\psi$). The presence of a $\Delta\psi$ may promote the insertion of the surface-bound pediocin molecules and stimulate the formation of more pore complexes and possibly bigger pores. A similar mechanism has been proposed for $\Delta\psi$-stimulated CF leakage from lipid vesicles caused by nisin (17) and channel formation caused by gallidermin and epidermin in black lipid membranes (6).

Pediocin PA-1 did permeablize the membrane of *Listeria* lipid vesicles in the absence of a transmembrane potential. This is in agreement with the in vivo observation that pediocin PA-1 dissipates proton motive force of *L. monocytogenes* cells in an energy-independent fashion (8). Nonetheless, the generation of a membrane potential (inside negative) stimulated the action of pediocin PA-1. Energy-enhanced action has also been shown for bavaricin MN on *Listeria* lipid vesicles (27), magainin 2 against acidic phospholipids (36, 38), and nisin-induced CF leakage from the zwitterionic phosphatidylcholine vesicles (17). A threshold membrane potential (inside negative) is required for nisin pore formation in the anionic phosphatidylglycerol (PG) vesicles (16).

It has been suggested that nisin has anionic carrier activity at low [peptide]/[lipid] ratio in highly defined zwitterionic phosphatidylcholine vesicles and that the carrier mode of action is inhibited by PG (16). Results from this study are inconsistent with a carrier mode of action for pediocin PA-1 for several reasons. The *Listeria* lipid vesicles are rich in anionic phospholipids and do not contain zwitterionic phospholipids (56). In the complex *Listeria* lipid vesicle system, which consists of at least five types of membrane lipids, the presence of PG does not inhibit the action of nisin (53), bavaricin MN (27), or pediocin PA-1. It is well established that pore formation is the mechanism by which pediocin PA-1 kills sensitive cells where efflux of intracellular solutes bearing positive, negative, or neutral charges occurs (1, 9, 10, 25, 28). Our previous study (9) shows that in *L. monocytogenes* cells, at 10 AU of pediocin PA-1 per ml, 25% of the intracellular P_i and maximal intracellular K^+ were lost over 10 min. At a similar pediocin concentration, i.e., 1.36 µM, which is 10 AU/ml, CF efflux from the *Listeria* lipid vesicles was of a magnitude similar to that of the P_i efflux—about 18% at 10 min. The comparable activities of pediocin PA-1 both in vitro and in vivo for positively and negatively charged molecules suggest a pore formation mechanism for pediocin PA-1-induced CF leakage from the lipid vesicles and are inconsistent with a carrier mechanism. Moreover, pore formation for nisin requires a threshold level of membrane potential (16), while pediocin PA-1 and other class IIa bacteriocins such as bavaricin MN and lactococcin A, which have chemical structures very different from that of nisin, act in an energy-independent fashion: they dissipate proton motive
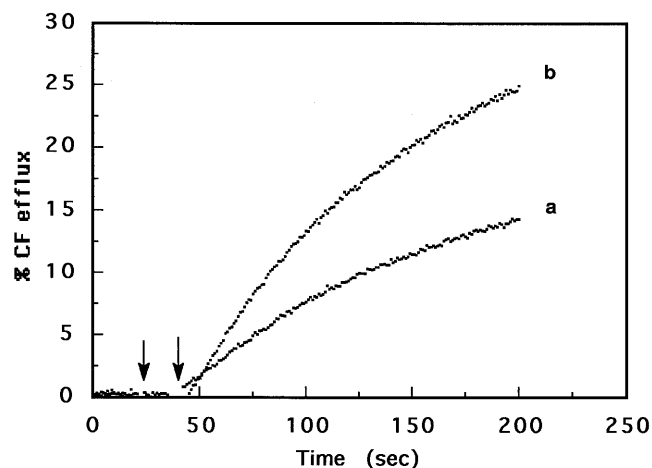

FIG. 6. Effect of an imposed transmembrane potential on pediocin-induced CF efflux from *Listeria* lipid vesicles at pH 6.0: 0 mV (a) and -120 mV (b). The first and second time arrows indicate the additions of valynomycin (2.5 µM) and pediocin PA-1 (6.3 µg/ml), respectively.

TABLE 2. Alignments by the Smith-Waterman algorithm of pediocin PA-1 with the SwissProt database

Bacteriocin	SwissProt entry no.	% Identity	Amino acid sequence[a]
Pediocin PA-1	P29430	100	**KYYGNGV**TCGKHS**C**SVDWGK**A**TTCIINN**G**AMAW**ATGG**HQ**G**NHKC
Pisciolin 126	P80569	56	**KYYGNGV**SCNKNGCTVDW**S**KAIGIIGNNAAANLTT**GG**AAGWNKG
Sakacin P	P35618	48	**KYYGNGV**HCGKHS**C**TVDW**G**TAI...GNI**G**NNAA**A**NWATGWNAGG
Leucocin A	P34034	46	**KYYGNGV**HCTKSGC**S**VNWGEAF....SAGVHRL**A**N**GG**NGFW
Mesentericin Y105	P38577	46	**KYYGNGV**HCTKSGC**S**VNWGEAA....SAGIHRL**A**N**GG**NGF
Bavaricin MN	P80493	38	T**KYYGNGV**YXNSKKXW**VDWG**QA**A**GGIGQTVVXGWLGGAIPGK
Carnobacterticin B2	P38580	36	VN**YGNGV**SC**S**KTK**C**S**VNWG**QAFQERYTA**GI**NSFVS**G**VAS**G**AGSIGRRP
Sakacin A	P80097	30	RS**YGNGV**YCNNKKCWVNR**G**EAT....QSIIGGMISGWAS**G**LAGM
Carnobacterticin BM1	P38579	27	IS**YGNGV**YCNKEKCWVNKAENKQAITGIVIGGW**A**SSLAGMGH

[a] Consensus amino acids are in boldface; dots indicate gaps introduced to maximize alignment.

force and induce efflux of intracellular solutes in the absence of a membrane potential (1, 8, 27, 52). Furthermore, the presence of a membrane potential enhances the activities of bavaricin MN in vitro (increasing CF efflux) and in vivo (increasing proton motive force dissipation) by similar magnitude (27), which independently verifies that the *Listeria* lipid vesicles system is a valid model for in vivo action. The $\Delta\psi$-mediated increase in CF efflux for pediocin PA-1 (88%) was similar to that for bavaricin MN (66%), while in the case of carrier activity of nisin, $\Delta\psi$ increases CF efflux by 250% in phosphatidylcholine vesicles (16).

Three-dimensional model for pediocin PA-1. A search by the Smith-Waterman algorithm (51) through the SwissProt database (44) resulted in a good alignment of the entire pediocin PA-1 sequence to other class IIa bacteriocins (Table 2). Pisciolin 126, sakacin P, and leucocin A had 56, 48, and 46% identity, respectively, to pediocin PA-1. There is overall agreement between the alignment presented in Table 2 and the alignment generated by Fasta and Blast (3, 44) for the 19 N-terminal amino acids of pediocin PA-1. The sequence similarities with other bacteriocins were low for the remaining 25 amino acids.

All methods used to predict secondary structure (13, 18, 19, 29, 31, 47) identified three short β-strands in the pediocin PA-1 sequence at approximately the same position. A consensus secondary structure prediction, based on all the methods, is presented in Table 3. Notably, most prediction methods agree that the sequence fragments containing Cys-9 and Cys-14 form two β-strands, connected by a short loop or turn. This is in agreement with the results of NMR data for leucocin A, which show an ordered β-structure only in the vicinity of the cysteines (49). Biochemical studies suggest that the cysteine side chains are linked by a disulfide bridge (25).

None of the threading programs (26, 50) found a significant match with a high Z score for the entire pediocin PA-1 sequence. Yet there appears to be a consensus that the tertiary structure predicted for the first 19 amino acids consists of two β-strands connected by cysteines to form a β-hairpin. This putative three-dimensional structure is consistent with the predictions generated by the secondary-structure methods and with the biochemical evidence showing that Cys-9 and Cys-14 form a disulfide bridge (25). A model (Fig. 7) consistent with these results was built for the 19 N-terminal amino acids of pediocin PA-1, and it was subjected to energy minimization by using the Encad program (32). The model consists of two β-strands connected by a tight 4-residue β-turn (β-hairpin). The N-terminal β-turn, YGNGV, is highly conserved in other class IIa bacteriocins and also occurs in several other proteins found in the Protein Data Bank (2, 7), including diphtheria toxin 1DDT (5, 11). In addition, disulfides on the adjacent β-strands have been observed experimentally in the structure of the human receptor for human immunodeficiency virus CD4 (48). The tip of the β-hairpin contains two positively charged residues (Lys-11 and His-12). Because of its high degree of conformational freedom, no structure could be predicted for the carboxy terminus of pediocin PA-1. However, the C24-C44 disulfide bond is required for pediocin activity (9, 10). This disulfide bond would bring together His-42, Lys-43, and possibly Lys-20 to create another positive patch. Reducing the disulfide bonds would disrupt the positive patches and would weaken the electrostatic interaction with anionic phospholipids. The existence of these positive patches in the three-dimensional model is consistent with the argument that electrostatic interaction plays an important role in the binding of pediocin PA-1 to *Listeria* lipid vesicles which contain anionic phospholipids. Our model also predicts the existence of a hydrophobic patch, consisting of residues Val-7, Cys-9, Cys-14, Val-16, and

TABLE 3. Secondary-structure prediction of pediocin PA-1

Method	Sequence and secondary structure[a]	Reference
	KYYGNGVTCGKHSCSVDWGKATTCIINNGAMAWATGGHQGNHKC	
PHD	EEE E HHHHHHHHHHHHEE	47
Gibrat	EE EEEEE E EEEEEEH EEEEH EE	19
Levine	EEE EE E EE EEEE	31
DPM	E E HEEEEE HHHHH	13
SOPMA	EEE E EEEE HEE E HHH	18
Nnpredict	EE EEEH HHHH	29
Consensus	.E....EEE.....EE	

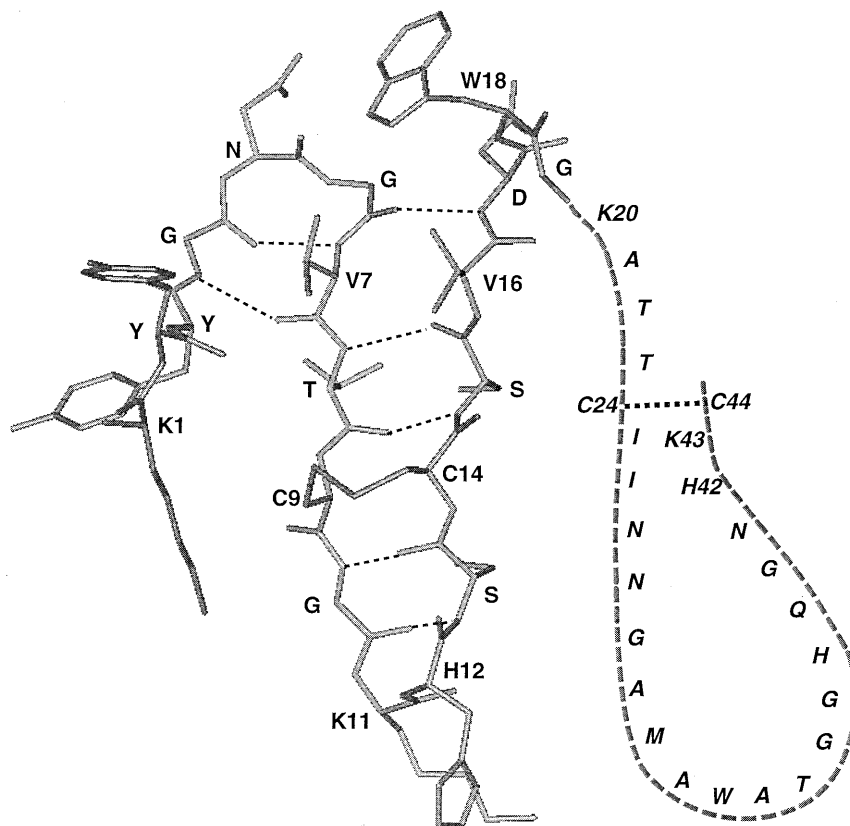[a] H, α-helix; E, β-sheet; dots, gaps to maximize alignment.

FIG. 7. Predicted three-dimensional model for the tertiary structure of pediocin PA-1's 19 N-terminal amino acids. The sequence of residues 20 to 44 is indicated without a structure except for the C24-C44 disulfide bond required for activity.

Trp-18. This hydrophobic patch may be important for the insertion of the pediocin PA-1 molecule into the membrane.

In conclusion, results from this study add new insight to the action of pediocin PA-1 by showing that it permeablized lipid vesicles in the absence of a membrane protein. Whether the presence of the previously postulated protein receptor would increase the binding of pediocin PA-1 to target membranes or plays a role in its subsequent insertion in the membrane has yet to be determined. Physicochemical characterization of the pediocin-membrane interaction revealed that the binding affinity for pediocin PA-1 to the membrane of *Listeria* lipid vesicles was higher than that for nisin, probably due to a stronger electrostatic interaction. Sequence alignments and secondary-structure predictions for the amino acids of pediocin PA-1 and other members of the class IIa bacteriocins suggested the existence of two β-strands which form a hairpin stabilized by a disulfide bridge in the N terminus.

REFERENCES

1. **Abee, T.** 1995. Pore-forming bacteriocins of Gram-positive bacteria and self-protection mechanisms of producer organisms. FEMS Microbiol. Lett. **129:**1–10.

2. **Abola, E., F. C. Bernstein, S. H. Bryant, T. F. Koetzle, and J. Wang.** 1987. Protein data bank, p. 107–132. *In* F. H. Allen, G. Bergerhoff, and R. Sievers (ed.), Data Commission of the International Union of Crystallography. International Union of Crystallography, Cambridge, United Kingdom.

3. **Altschul, S. F., W. Gish, W. Miller, E. W. Myers, and D. J. Lipman.** 1990. Basic local alignment search tool. J. Mol. Biol. **215:**403–410.

4. **Aymerich, T., H. Holo, L. S. Havarstein, M. Hugas, M. Garriga, and I. F. Nes.** 1996. Biochemical and genetic characterization of enterocin A from *Enterococcus faecium*, a new antilisterial bacteriocin in the pediocin family of bacteriocins. Appl. Environ. Microbiol. **62:**1676–1682.

5. **Bennett, M. J., S. Choe, and D. Eisenberg.** 1994. Domain swapping: entangling alliances between proteins. Proc. Natl. Acad. Sci. USA **91:**3127–3131.

6. **Bens, R., G. Jung, and H.-G. Shal.** 1991. Mechanism of channel formation by lantibiotics in black lipid membranes. p. 359–372. *In* G. Jung and H.-G. Salh (ed.), Nisin and novel lantibiotics. Escom Publishers, Leiden, The Netherlands.

7. **Bernstein, F. C., T. F. Koetzle, G. J. B. Williams, E. F. Meyer, Jr., M. D. Brice, J. R. Rodgers, O. Kennard, T. Shimanouchi, and M. Tasumi.** 1977. The protein data bank: a computer-based archive file for macromolecular structures. J. Mol. Biol. **112:**535–542.

8. **Bruno, M. E. C., and T. J. Montville.** 1993. Common mechanistic action of bacteriocins from lactic acid bacteria. Appl. Environ. Microbiol. **59:**3003–3010.

9. **Chen, Y., and T. J. Montville.** 1995. Efflux of ions and ATP depletion induced by pediocin PA-1 are concomitant with cell death in *Listeria monocytogenes* Scott A. J. Appl. Bacteriol. **79:**684–690.

10. **Chikindas, M. L., M. J. Garcia-Garcera, A. J. M. Driessen, A. M. Ledeboer, J. Nissen-Meyer, I. F. Nes, T. Abee, W. N. Konings, and G. Venema.** 1993. Pediocin PA-1, a bacteriocin from *Pediococcus acidilactici* PAC 1.0, forms hydrophilic pores in the cytoplasmic membrane of target cells. Appl. Environ. Microbiol. **59:**3577–3584.

11. **Choe, S., M. J. Bennett, G. Fujii, P. M. G. Curmi, K. A. Kantardjieff, R. J. Collier, and D. Eisenberg.** 1992. The crystal structure of diphtheria toxin. Nature **357:**216–222.

12. **Cruciani, R. A., J. L. Barker, S. R. Durell, G. Raghunathan, H. R. Guy, M. Zasloff, and E. F. Stanley.** 1992. Magainin 2, a natural antibiotic from frog skin, forms ion channels in lipid bilayer membranes. Eur. J. Pharmacol. **226:**287–296.

13. **Deleage, G., and B. Roux.** 1987. An algorithm for protein secondary structure prediction based on class prediction. Protein Eng. **1:**289–294.
14. **Demel, R. A., T. Peelen, R. J. Siezen, B. de Kruijff, and O. P. Kuipers.** 1996. Nisin Z, mutant nisin Z and lacticin 481 interactions with anionic lipids correlate with antimicrobial activity, a monolayer study. Eur. J. Biochem. **235:**267–274.
15. **Driessen, A. J. M., and W. N. Konings.** 1993. Insertion of lipids and proteins into bacterial membranes by fusion with liposomes. Methods Enzymol. **221:**394–408.
16. **Driessen, A. J. M., H. W. van den Hooven, W. Kuiper, M. van de Kamp, H.-G. Sahl, R. N. H. Konings, and W. N. Konings.** 1995. Mechanistic studies of lantibiotic-induced permeabilization of phospholipid vesicles. Biochemistry **34:**1606–1614.
17. **García-Garcerá, M. J., M. G. L. Elferinc, A. J. M. Driessen, and W. N. Konings.** 1993. In vitro pore-forming activity of the lantibiotic nisin: role of the proton motive force and lipid composition. Eur. J. Biochem. **212:**417–422.
18. **Geourjon, C., and G. Deleage.** 1995. Antheprot: a software to display and analyze 3D NMR structures. Trace Microprob. Tech. **13:**337–338.
19. **Gibrat, J. F., J. Garnier, and B. Robson.** 1987. Further developments of protein secondary structure prediction using information theory: new parameters and consideration of residue pairs. J. Mol. Biol. **198:**425–443.
20. **Gonzalez, C. F.** 1988. Method for inhibiting bacterial spoilage and composition for this purpose. European patent application 88101624.
21. **Grant, E., Jr., T. J. Beeler, K. M. P. Taylor, K. Gable, and M. A. Roseman.** 1992. Mechanism of magainin 2a induced permeabilization of phospholipid vesicles. Biochemistry **31:**9912–9918.
22. **Hastings, J. W., M. Sailer, K. Johnson, K. L. Roy, J. C. Vederas, and M. E. Stiles.** 1991. Characterization of leucocin A-UAL 187 and cloning of the bacteriocin gene from *Leuconostoc gelidum*. J. Bacteriol. **173:**7491–7500.
23. **Henderson, J. T., A. L. Chopko, and P. D. van Wassenaar.** 1992. Purification and primary structure of pediocin PA-1 produced by *Pediococcus acidilactici* PAC-1.0. Arch. Biochem. Biophys. **295:**5–12.
24. **Huis in't Veld, J. H. J.** 1995. Use of bacteriocins to preserve foods, abstr. 2.1. Workshop on the bacteriocins of lactic acid bacteria: applications and fundamentals, Alberta, Canada.
25. **Jack, R. W., J. R. Tagg, and B. Ray.** 1995. Bacteriocins of Gram-positive bacteria. Microbiol. Rev. **59:**171–200.
26. **Jones, D. T., W. R. Taylor, and J. M. Thornton.** 1992. A new approach to protein fold recognition. Nature **358:**86–89.
27. **Kaiser, A. L., and T. J. Montville.** 1996. Purification of the bacteriocin bavaricin MN and characterization of its mode of action against *Listeria monocytogenes* Scott A cells and lipid vesicles. Appl. Environ. Microbiol. **62:**4529–4535.
28. **Klaenhammer, T. R.** 1993. Genetics of bacteriocins produced by lactic acid bacteria. FEMS Microbiol. Rev. **12:**39–86.
29. **Kneller, D. G., F. E. Cohen, and R. Langridge.** 1990. Improvement in protein secondary structure prediction by an enhanced neural network. J. Mol. Biol. **214:**171–182.
30. **Leistner, L.** 1994. Principles and applications of hurdle technology, p. 1–21. *In* G. W. Grould (ed.), New methods of food preservation. Blackie Academic and Professional, Glasgow, Scotland.
31. **Levin, J. M., B. Robson, and J. Garnier.** 1986. An algorithm for secondary structure determination in proteins based on sequence similarity. FEBS Lett. **205:**303–308.
32. **Levitt, M.** 1983. Molecular dynamics of native protein. I. Computer simulation of trajectories. J. Mol. Biol. **168:**595–620.
33. **Lian, L. Y., W. C. Chan, S. D. Morley, G. C. K. Roberts, B. W. Bycroft, and D. Jacson.** 1991. NMR studies of the solution structure of nisin A and related peptides, p. 43–58. *In* G. Jung and H.-G. Sahl (ed.), Nisin and novel lantibiotics. Escom Publishers, Leiden, The Netherlands.
34. **Maftah, A., D. Renault, C. Vignoles, Y. Héchard, P. Bressolier, M. H. Ratinaud, Y. Cenatiempo, and R. Julien.** 1993. Membrane permeabilization of *Listeria monocytogenes* and mitochondria by bacteriocin mesentericin Y105. J. Bacteriol. **175:**3232–3235.
35. **Marugg, J. D., C. F. Gonzalez, B. S. Kunka, A. M. Ledeboer, M. J. Pucci, M. Y. Toonen, S. A. Walker, L. C. M. Zoetmulder, and P. A. Vandenbergh.** 1992. Cloning, expression, and nucleotide sequence of genes involved in production of pediocin PA-1, a bacteriocin from *Pediococcuc acidilactici* PAC1.0. Appl. Environ. Microbiol. **58:**2360–2367.
36. **Matsuzaki, K., K. Sugishita, N. Fujii, and K. Miyajima.** 1995. Molecular basis for membrane selectivity of an antimicrobial peptide, magainin 2. Biochemistry **34:**3423–3429.
37. **Matsuzaki, K., M. Harada, T. Handa, S. Funakoshi, N. Fujii, H. Yajima, and K. Miyajima.** 1989. Magainin 1-induced leakage of entrapped calcein out of negatively-charged lipid vesicles. Biochim. Biophys. Acta **981:**130–134.
38. **Matsuzaki, K., O. Murase, N. Fujii, and K. Miyajima.** 1995. Translocation of a channel-forming antimicrobial peptide, magainin 2, across lipid bilayers by forming a pore. Biochemistry **34:**6521–6526.
39. **Montville, T. J., and K. Winkowski.** 1997. Biologically-based preservation systems and probiotic bacteria, p. 557–577. *In* M. P. Doyle, L. R. Beuchat, and T. J. Montville (ed.), Food microbiology: fundamentals and frontiers. American Society for Microbiology Press, Washington, D.C.
40. **Motlagh, A. M., A. K. Bhunia, F. Szostek, T. R. Hansen, M. C. Johnson, and B. Ray.** 1992. Nucleotide and amino acid sequence of pap-gene (pediocin AcH production) in *Pediococcus acidilactici* H. Lett. Appl. Microbiol. **15:**45–48.
41. **New, R. R. C.** 1992. Characterization of liposomes, p. 105–162. *In* R. R. C. New (ed.), Liposomes: a practical approach. IRL Press, Oxford, England.
42. **Ojcious, D. M., and J. D. E. Young.** 1991. Cytoplasmic pore forming proteins and peptides: is there a common structural motif? Trends Biochem. Sci. **16:**225–229.
43. **Palmer, D. E., D. F. Mierke, C. Pattaroni, M. Goodman, T. Wakamiya, K. Fukase, M. Kitazawa, H. Fujita, and T. Shiba.** 1989. Interactive NMR and computer simulation studies of lanthionine-ring structures. Biopolymers **28:**397–408.
44. **Pearson, W. R., and D. J. Lipman.** 1988. Improved tools for biological sequence comparison. Proc. Natl. Acad. Sci. USA **85:**2444–2448.
45. **Pucci, M. J., E. R. Vedamuthu, B. S. Kunka, and P. A. Vandenberg.** 1988. Inhibition of *Listeria monocytogenes* by using bacteriocin PA-1 produced by *Pediococcus acidilactici* PAC1.0. Appl. Environ. Microbiol. **54:**2349–2353.
46. **Quadri, L. E. N., M. Sailer, K. L. Roy, J. C. Venderas, and M. E. Stiles.** 1994. Chemical and genetic characterization of bacteriocins produced by *Carnobacterium piscicola* LV17B. J. Biol. Chem. **269:**12204–12211.
47. **Rost, B., and C. Sander.** 1994. Combining evolutionary information and neural networks to predict protein secondary structure. Proteins Struct. Funct. Gene. **19:**55–72.
48. **Ryu, S. E., A. Truneh, R. W. Sweet, and W. A. Hendrickson.** 1994. Structures of an HIV and MHC binding fragment from human CD4 as refined in two crystal lattices structure. Structure **2:**59–74.
49. **Sailer, M., G. L. Helms, T. Henkel, W. P. Niemczura, M. E. Stiles, and J. C. Vederas.** 1992. 15N- and 13C-labeled media from *Anabaena* sp. for universal isotopic labeling of bacteriocins: NMR resonance assignments of leucocin A from *Leuconostoc gelidum* and nisin A from *Lactococcus lactis*. Biochemistry **32:**310–318.
50. **Sippl, M. J., and S. Weitckus.** 1992. Detection of native-like models for amino acid sequences of unknown three-dimensional structure in a data base of unknown protein conformations. Proteins **13:**258–271.
51. **Smith, T. F., and M. S. Waterman.** 1981. Identification of common molecular subsequences. J. Mol. Biol. **147:**195–197.
52. **van Belkum, M. J., J. Kok, G. Venema, H. Holo, I. F. Nes, W. N. Konings, and T. Abee.** 1991. The bacteriocin lactococcin A specifically increases the permeability of lactococcal cytoplasmic membranes in a voltage-independent, protein-mediated manner. J. Bacteriol. **173:**7934–7941.
53. **Vandenbergh, P. A., M. J. Pucci, B. S. Kunka, and E. R. Vedamuthu.** 1989. Method for inhibiting *Listeria monocytogenes* using a bacteriocin. European patent application 89101125.6
54. **van de Ven, F. J. M., H. W. van den Hooven, R. N. H. Konings, and C. W. Hilbers.** 1991. The spatial structure of nisin in aqueous solution, p. 35–42. *In* G. Jung and H.-G. Sahl (ed.), Nisin and novel lantibiotics. Escom Publishers, Leiden, The Netherlands.
55. **Venema, K., G. Venema, and J. Kok.** 1995. Lactococcins: mode of action, immunity and secretion. Int. Dairy J. **5:**815–832.
56. **Winkowski, K., R. D. Ludescher, and T. J. Montville.** 1996. Physicochemical characterization of the nisin-membrane interaction with liposomes derived from *Listeria monocytogenes*. Appl. Environ. Microbiol. **62:**323–327.